SST anomalies related to wind stress curl patterns in the Japan/East Sea

Olga Trusenkova, Vyacheslav Lobanov, Dmitry Kaplunenko
V.I. Ilyichev Pacific Oceanological Institute, Russian Academy of Sciences,
43 Baltiyskaya St., Vladivostok, 690041, Russia

Motivation

<u>Local and non-local forcings for SST variability</u>

Studies for the JES focused on interannual to interdecadal timescales

Revealed are links of SSTA to:

- Siberian High related to Arctic and North Atlantic Oscillations
- North Pacific High
- Aleutian Low
- East Asia jet stream

→ *impact on local air – sea heat exchange* (Minobe et al., 2004; Park and Chu, 2006)

Local forcing can be also provided by C/AC wind stress curl:

- current divergence/convergence

Non-local mechanisms ~ heat advection by oceanic currents
heat fluxes caused by mesoscale dynamics

---

mesoscale dynamics in the JES ~ many studies

Availability of high-resolution daily SST datasets stimulates analysis of high frequency SST anomalies

Purpose of the study

To reveal dynamically induced SST anomalies in the Japan/East Sea (JES) from datasets with high spatial and temporal resolution

Data

Daily New Generation (NG) **SST**, Tohoku University, Sendai, Japan,
July 1, 2002 - July 7, 2006, 34.5°- 48°N, 127.5°- 142°E,
0.05°-gridded, smoothed to 0.25° for computational purposes,
satellite IR & MK

Daily Japan Meteorological Agency (JMA) **SST**,
October 12, 1993 – November 8, 2006, 35°- 48°N, 127.5°- 142°E,
0.25°-gridded, satellite IR & MK + *in situ*

NCEP/NCAR **wind**, 6h 1°x1° gridded surface fields,
1998-2005, 34°-53°N, 127°-143°E
(SeaWiFS Project Ancillary Data)

Complex EOF Analysis

$X(r, t) = \sum A_k(r)B_k(t)$,

where r stands for the spatial coordinates and t for time,

$X(r, t) = X_r(r, t) + iX_i(r, t)$,

$X_r(r, t)$ is real part (SST fields),

X_i is imaginary part calculated from Hilbert Transform,

$A_k(r) = \mathit{A}_k(r)e^{-i\varphi}$ is spatial CEOF,

$B_k(t) = \mathit{B}_k(t)e^{-i\phi}$ is temporal PC (principal component),

A_k / B_k is spatial/temporal amplitude,

φ_k / ϕ_k is spatial/temporal phase (-180°, 180°).

$X_a(r, t) = X(r, t) – A_1(r)B_1(t)$ is residual anomaly

$X_{a'}(r_0, t) = A_k(r_0)B_k(t)$ is CEOF k related anomaly in the r_0 location

$X_{a'}(r, t_0) = A_k(r)B_k(t_0)$ is CEOF k related anomaly for the time count t_0.

MHI oceanic model

(Shapiro and Mikhaylova, 1992-1998)

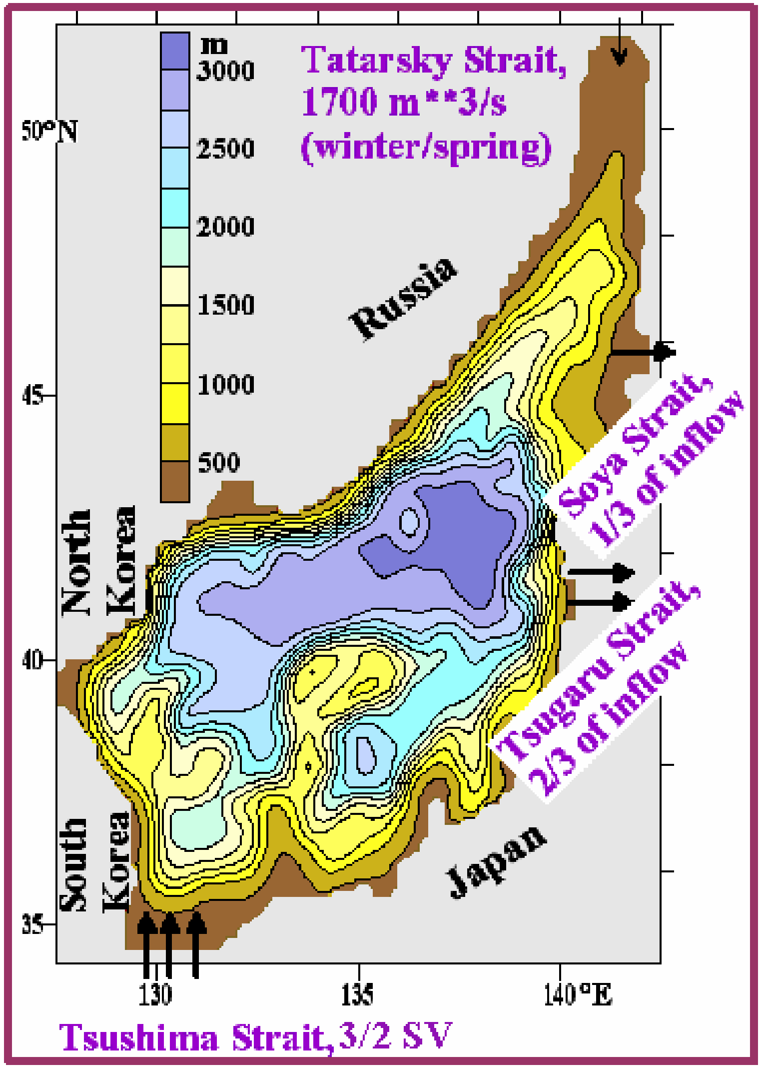

- 3D primitive equation, hydrostatic & Boussinesq
- Quasi-isopycnic co-ordinate in the vertical
- Complete thermodynamics, including
  - surface heat/freshwater balances,
  - TKE model for the surface mixed layer,
  - prognostic equations for T and S,
  - diapycnal exchange of T and S between the layers
- Variable T, S, and buoyancy in any layer
- Constraint on buoyancy variations in the inner layers (below the mixed layer)
- Bi-harmonic viscosity in the momentum equations
- Free surface
- Convective adjustment

Typical wind stress and curl patterns

(Trusenkova et al., 2007)

Winter monsoon

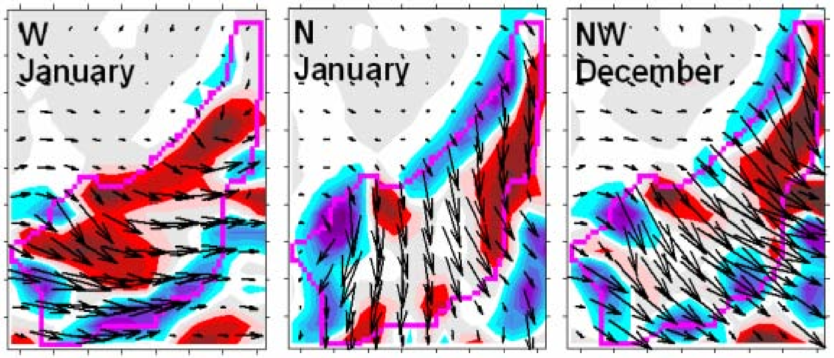

Summer monsoon, westerlies

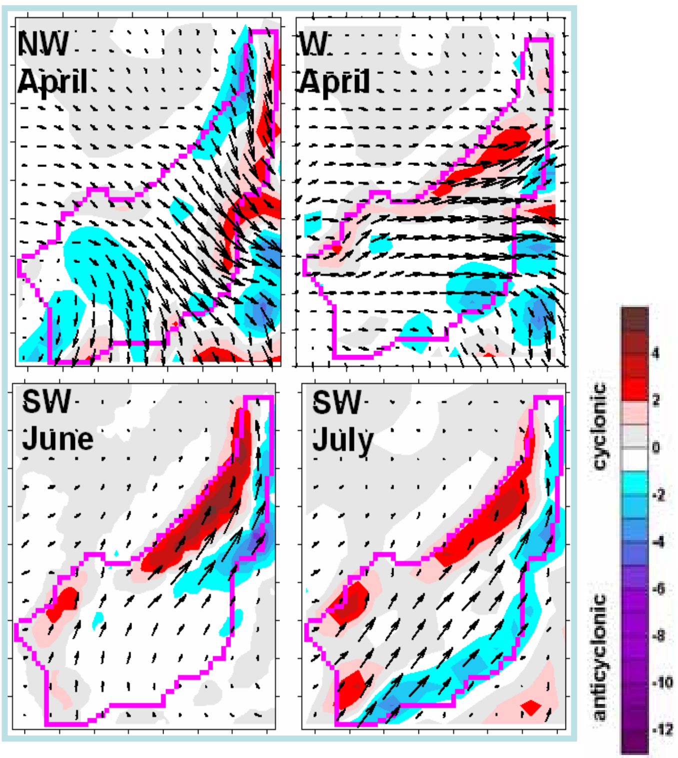

Vectors: dyne/cm^2
contours: $2x10^{-8}$ dyne/cm^3

Summer monsoon, easterlies

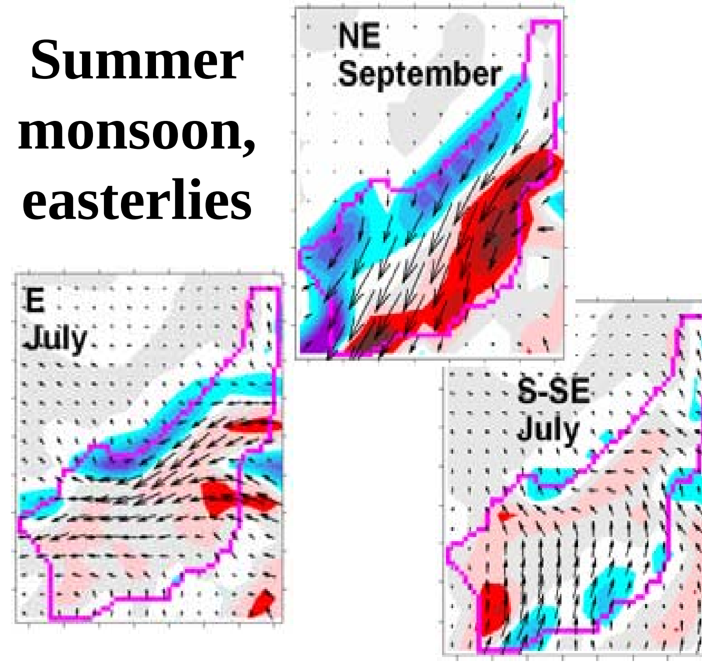

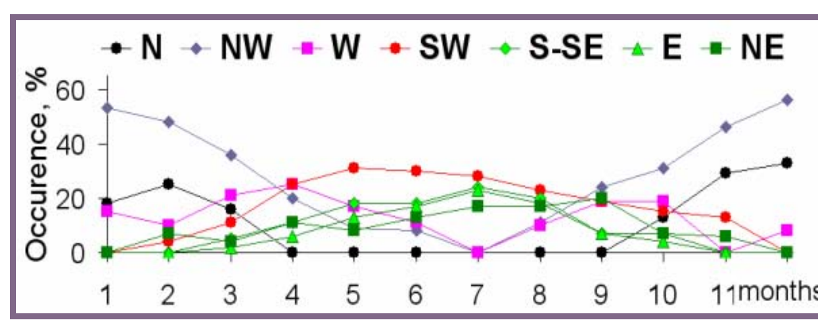

JMA SST decomposition, MODE 1: average annual cycle

Average annual cycle:
- homogeneous over the JES,
- minimum in February – March, maximum in August,
- asymmetry, with faster spring warming and slower autumn cooling;
- interannual variability due to air – sea heat exchange variations.

Mode 1 related anomaly:
$\mathbf{X_a}'(\mathbf{r}_0, t) = A_1(\mathbf{r}_0)B_1(t)$

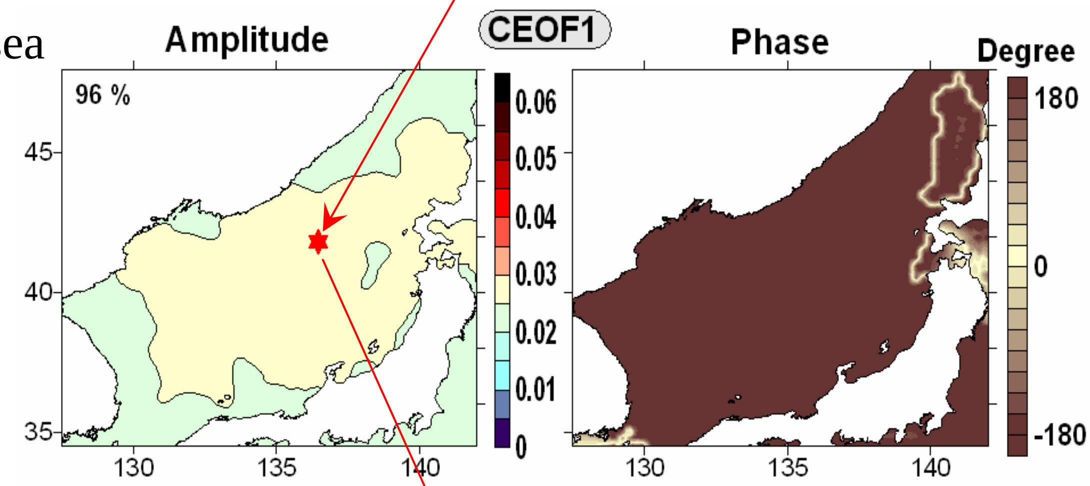

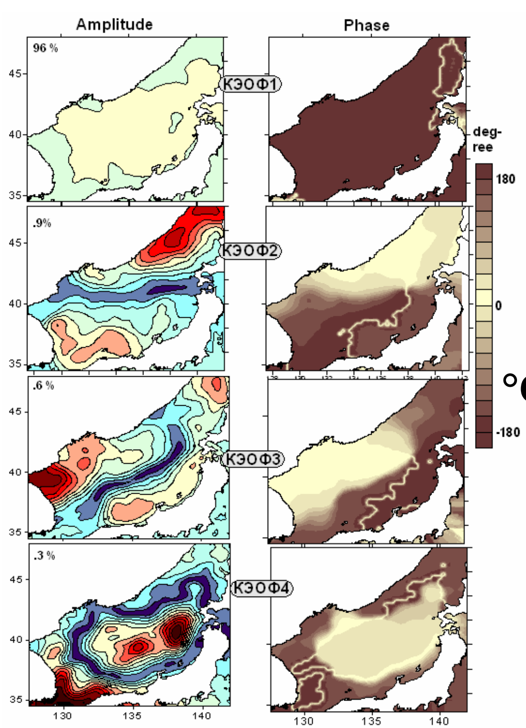

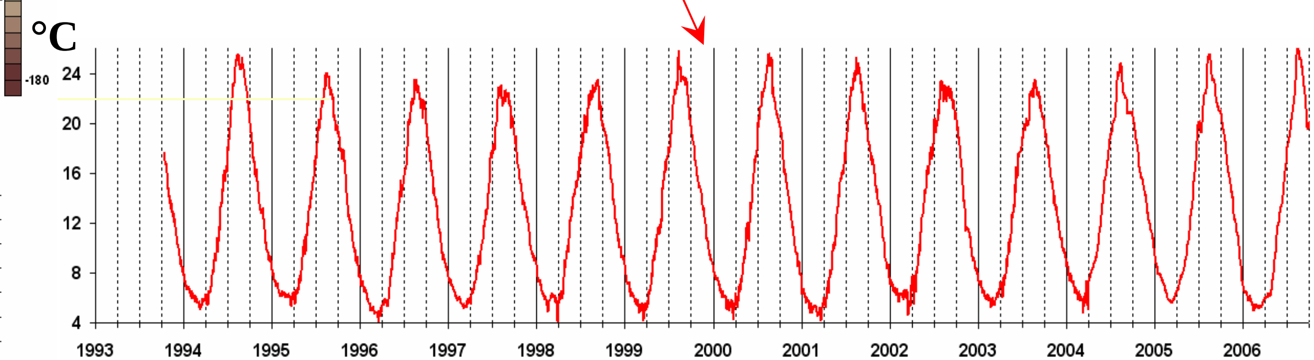

Surface heat forcing of the annual cycle: SSTA vs. T air and wind speed

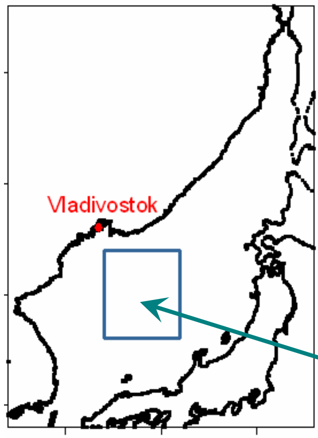

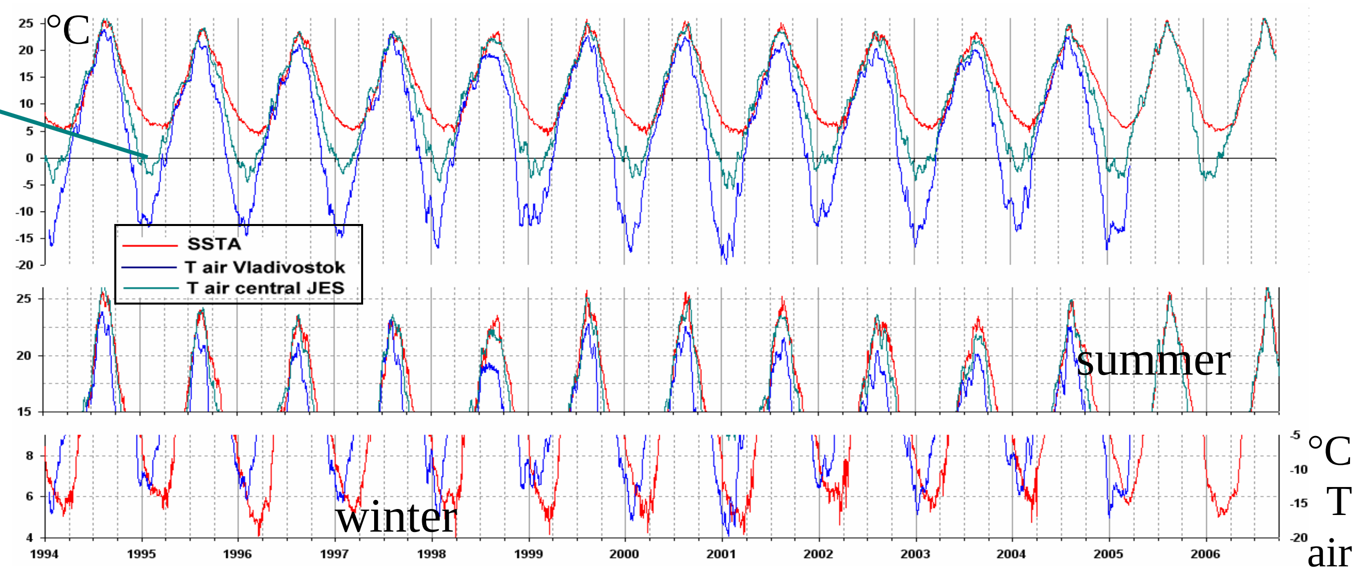

SSTA and T air linked in winter (lower T air, lower SST) and summer (greater T air, greater SST)

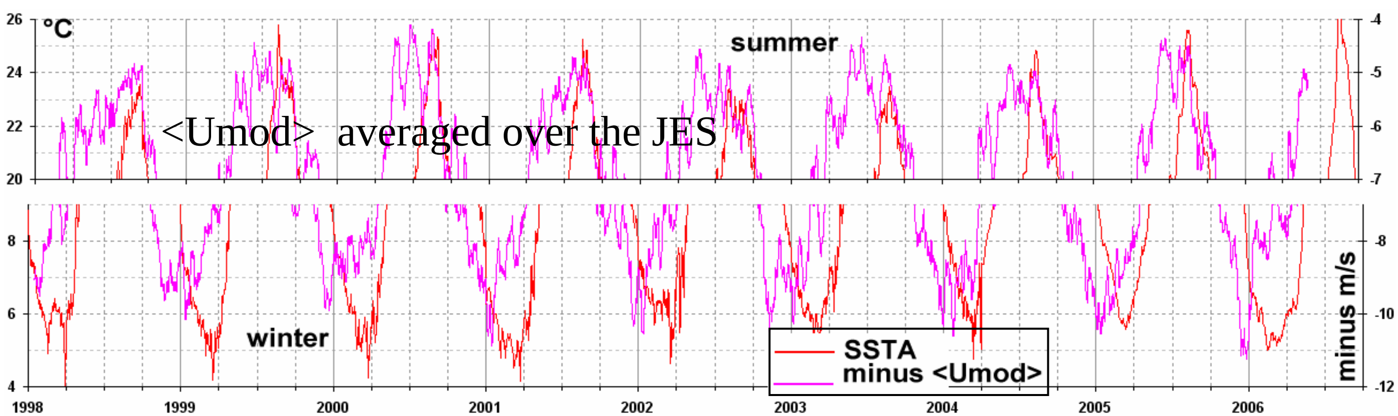

SSTA and wind speed linked in summer (stronger wind, lower SST), less evident in winter

Residual anomalies SSTA1: JMA vs. NG

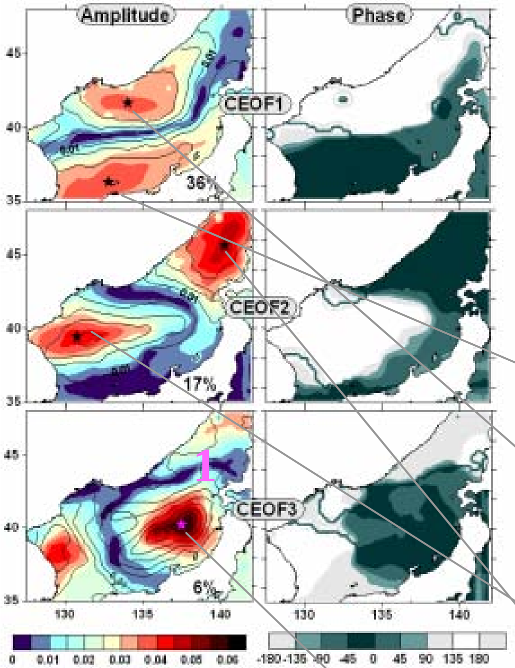

First order residual anomalies obtained by subtraction of the average annual cycle:
$\mathbf{X}_a^{(1)}(\mathbf{r}, t) = \mathbf{X}(\mathbf{r}, t) - A_1^{(0)}(\mathbf{r})B_1^{(0)}(t)$

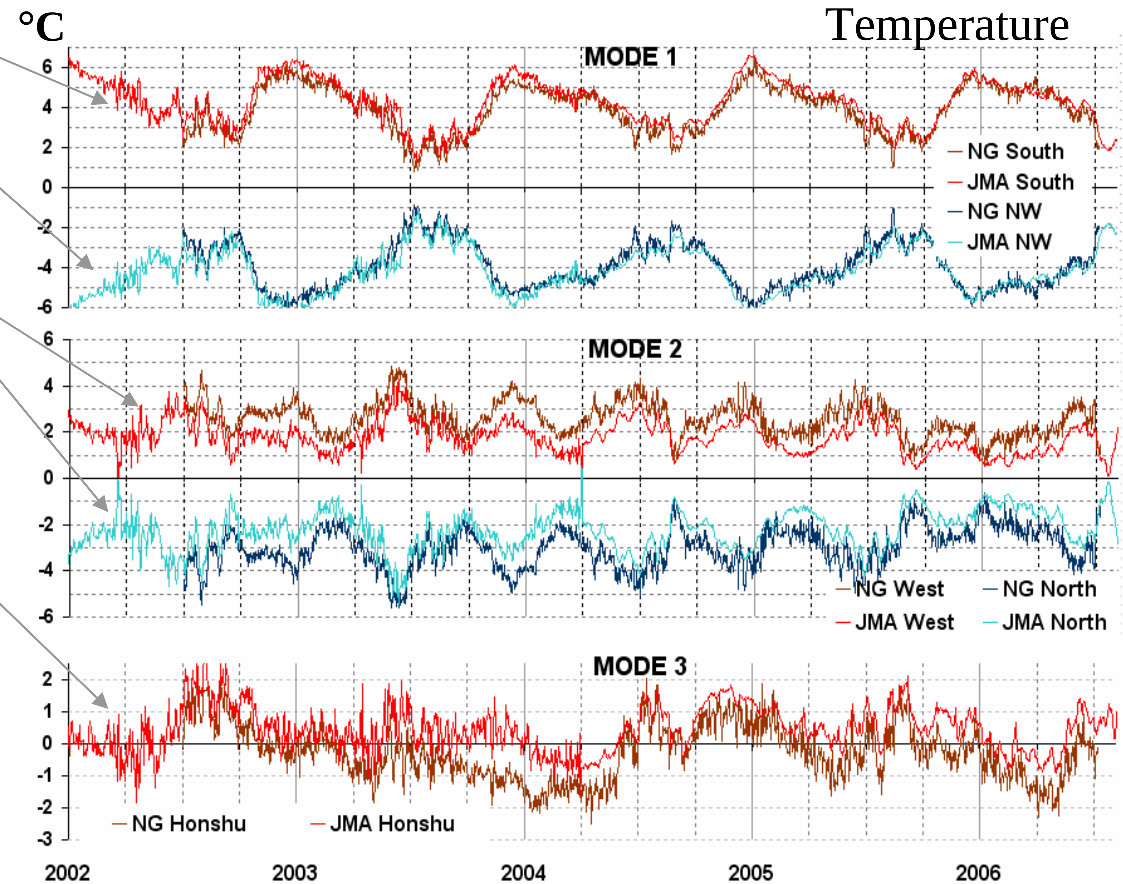

Amplitude:
JMA filled, NG contours

Phase for JMA, the same pattern for NG

The same pattern for Mode 1 & Mode 2

Some difference for Mode 3

JMA SSTA1: dominant time scales

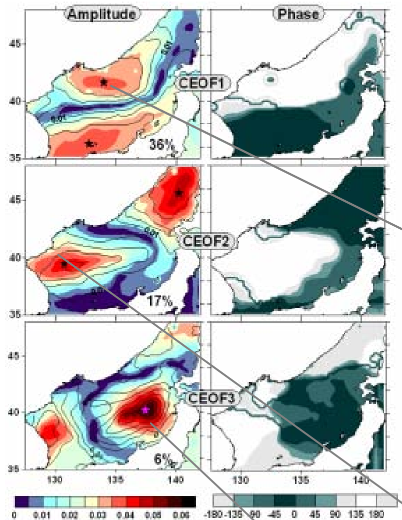

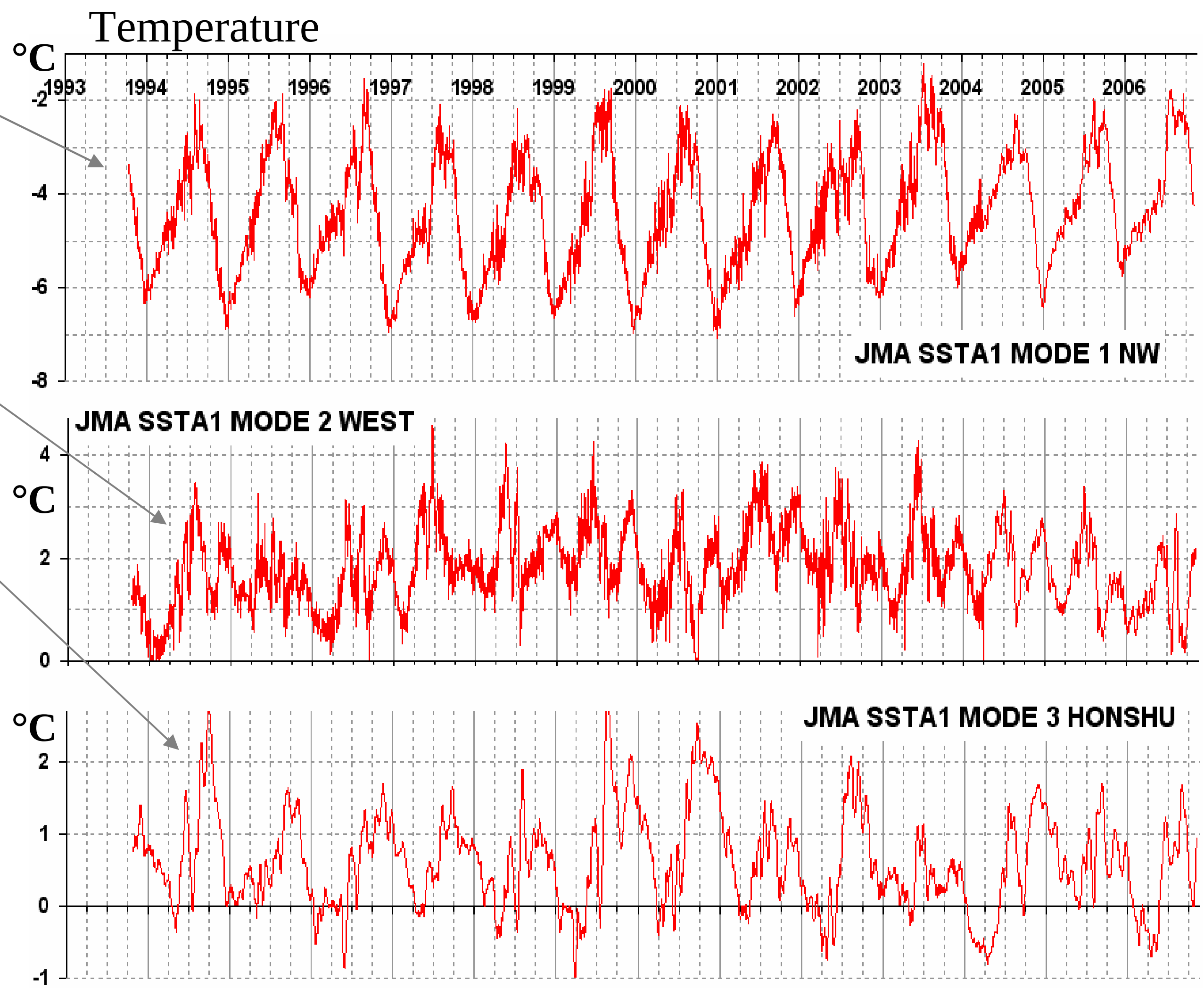

DOMINANT SCALES

Mode 1: 12 month scale, greatest in late December.

Mode 2: 6 month scale, greatest in May-June and November-December.

Mode 3: 12 month scale, greatest in July – October

NW core

Mode 1: adjustment to the annual cycle

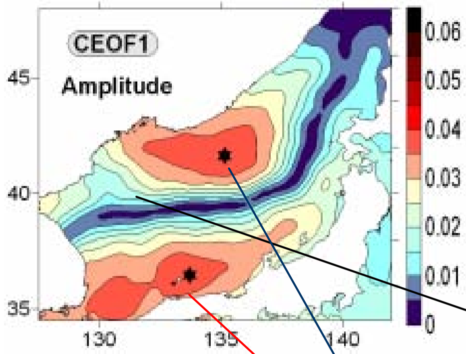

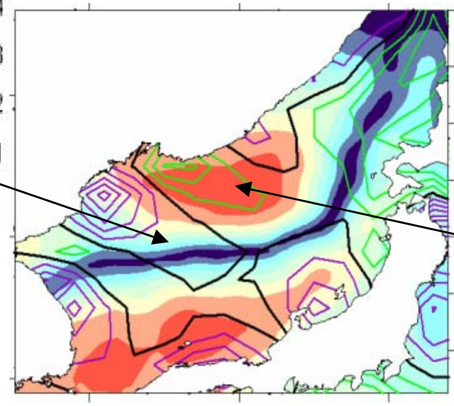

Wind stress & curl, December

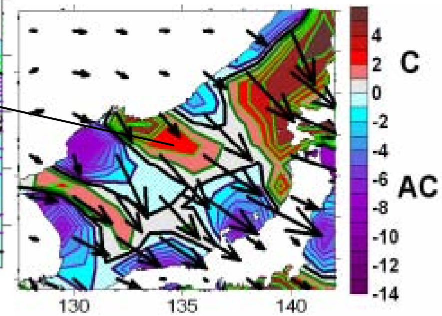

Wind speed, December

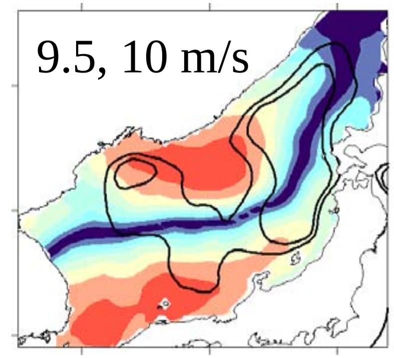

SSTA in the NW core related to wind stress curl but not to wind speed

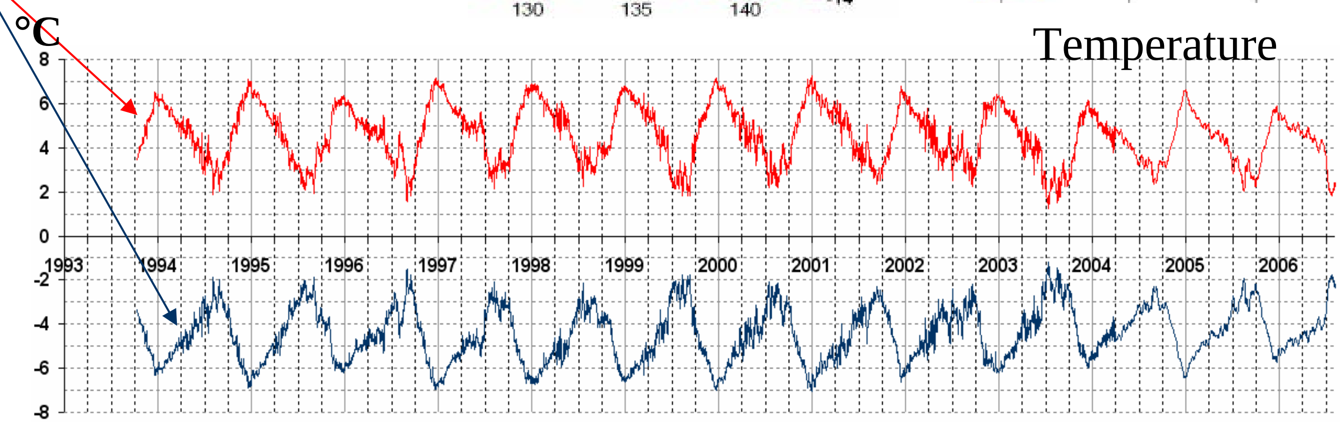

Greatest SSTA in late December

Southern core

related to subtropical water inflow in the Korea Strait.

Maximum transport: October-November (Takikawa, Yoon, 2005)

Southern and NW cores caused by different processes but with the similar temporal pattern, thus combined in the same mode

The simulated circulation in the NW JES in autumn - winter

Wind stress & curl, December

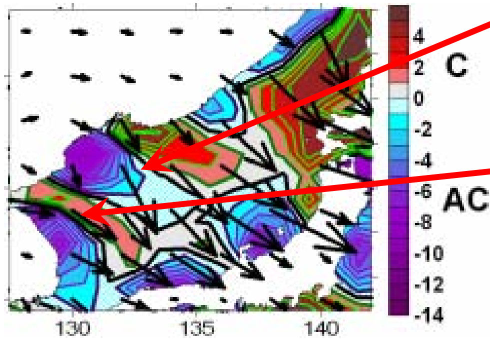

Curl dipole off Vladivostok

zone of C curl off East Korea Bay

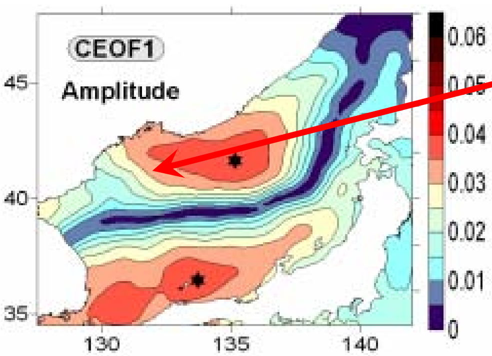

NW front
well known from satellite & ship observations (Danchenkov et al., 1997; Lobanov et al., 2001; Nikitin, 2002, 2006)

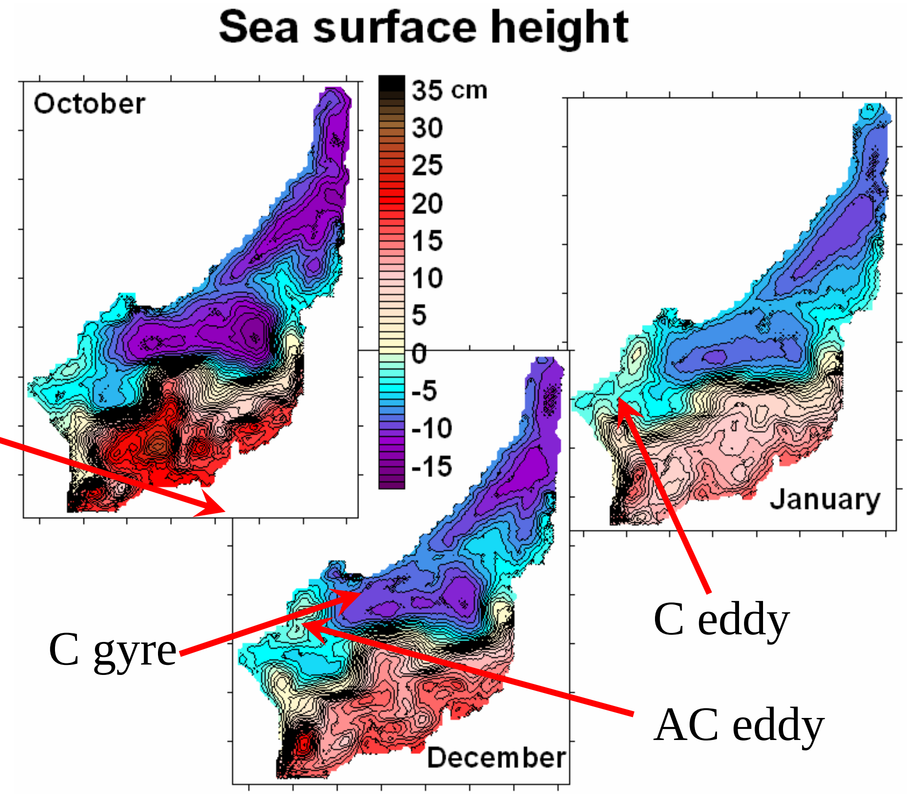

With the onset of winter monsoon in October, typical NW wind pattern forces C/AC circulation in the affected areas. Current divergence induces the SST decrease within C gyres/eddies.

Mode 2: semiannual periodicity

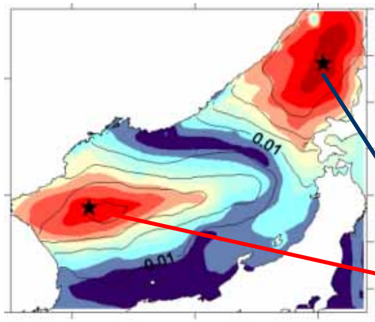

Temperature

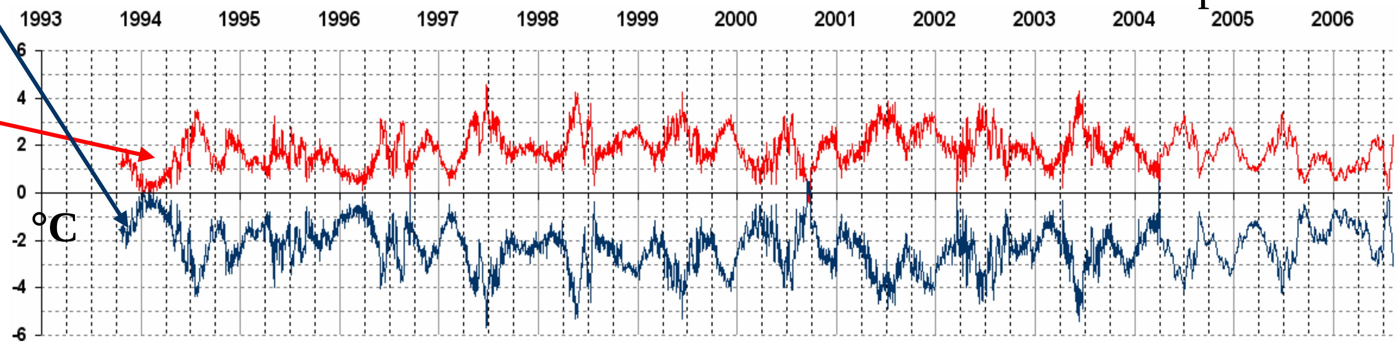

SSTA is the greatest in May-June & November-December,
the smallest in February-March & August-September

Semiannual oscillaions are revealed in:

- the JES SST, especially strong in the northern sea (Park and Chung, 1999);
- the JES surface height, especially strong in the western sea (Koldunov et al., 2007);
- transport in the Korea Strait (Takikawa and Yoon, 2005);
- the JES integral transport between Nakhodka and Naoetsu (Palshin et al., 2001);
- sea level presure, especially strong in the moderate and subtropical Northwest Pacific (Sedov, 1990).

Semiannual periodicity in wind stress curl

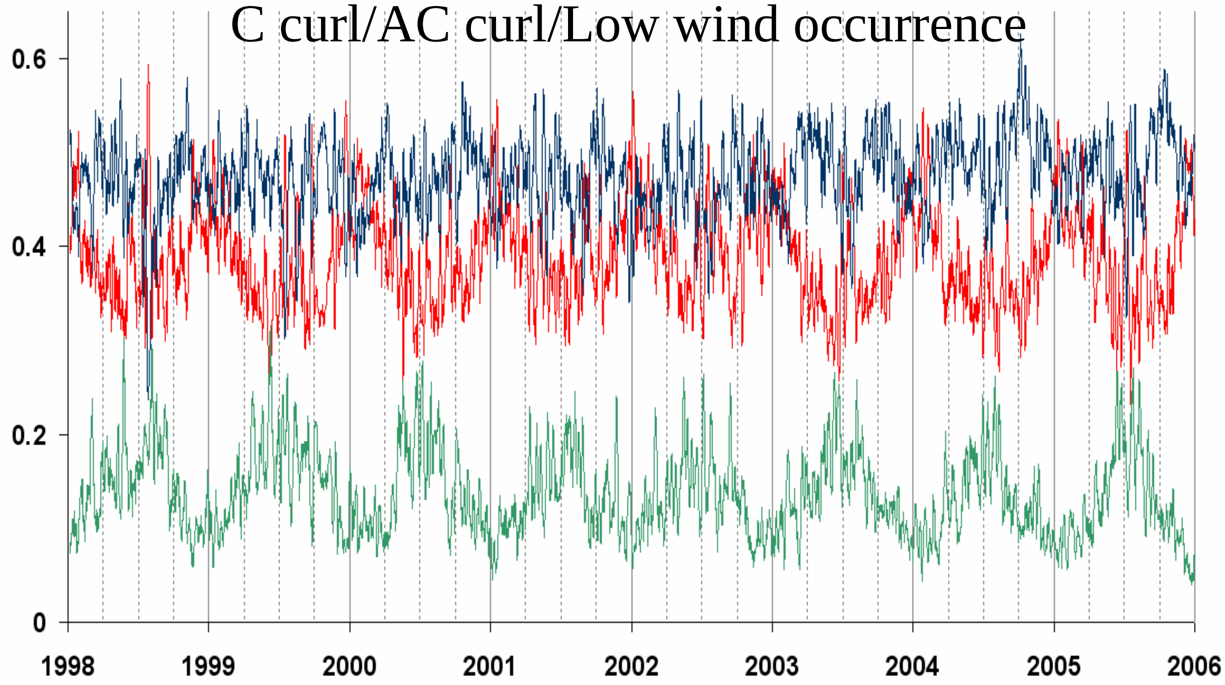

Occurrence: (portions of boxes over the JES):
a box adds to
C curl occurrence
if rotτ > C1;
AC curl occurrence
if rotτ < -C1;
Weak wind occurrence:
if -C1 < rotτ < C

$C1 = 0.5 \times 10^{-8}$ dyne/cm^3

AC curl (blue) max: April-June & September-October

C curl (red) max: winter, July-August

Weak wind (green)

- Opposition of C vs. AC curl occurrence (R = -0.67);
- Semiannual periodicity;
- Annual periodicity of the weak wind occurrence.

Mode 2, western core: links to wind stress curl

Lagged cross-correlation:
AC curl occurrence vs. SSTA

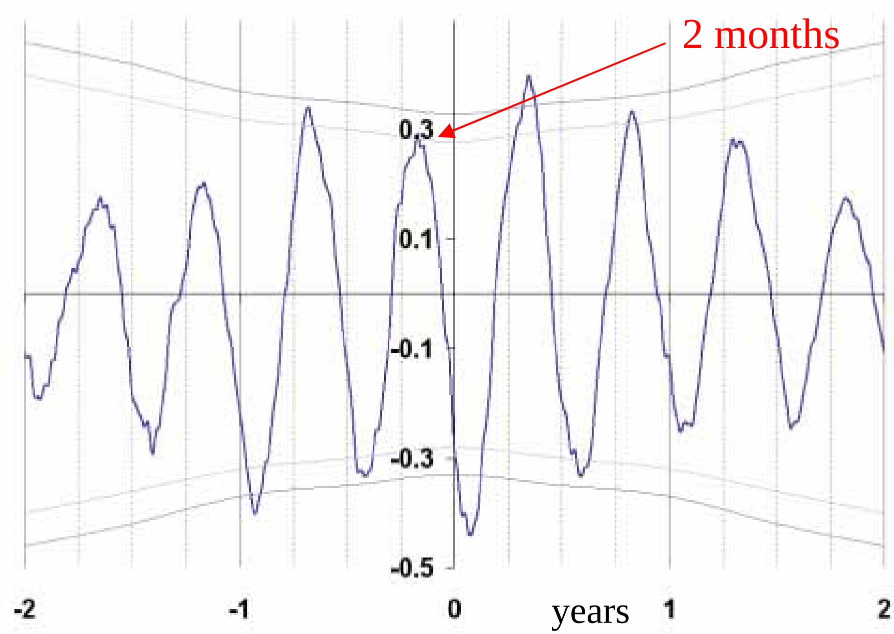

Wind leading SSTA leading

Semiannual timescale of the joint variability

Mode 2 – related SSTA in the western core lags 2 months behind the increased occurrence of the AC wind stress curl

Subarctic front seasonal variation and eddy formation

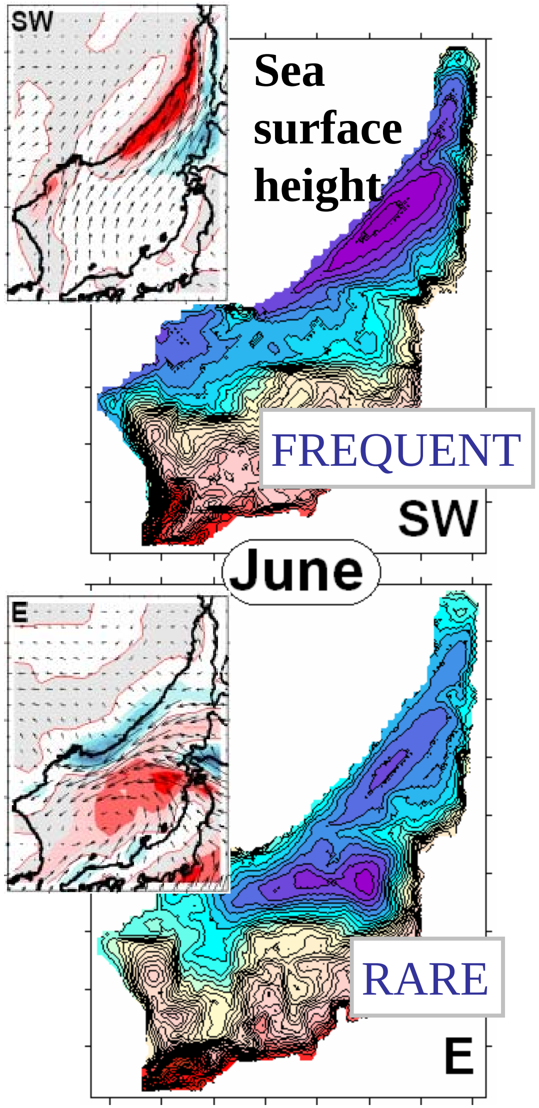

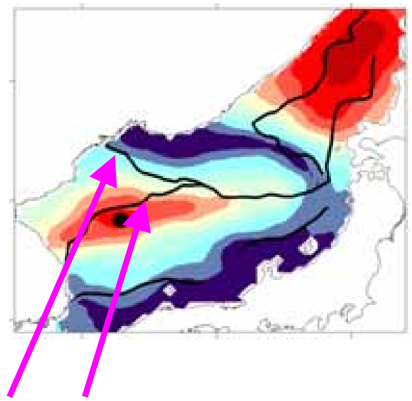

Northern shift of subarctic front in April-June (Nikitin, 2006)

The simulated circulation: northern shift of the western subarctic front under the forcing of wind with AC curl, frequent in June, thus positive SST anomaly. No shift under the forcing of the C curl (rare events in spring).

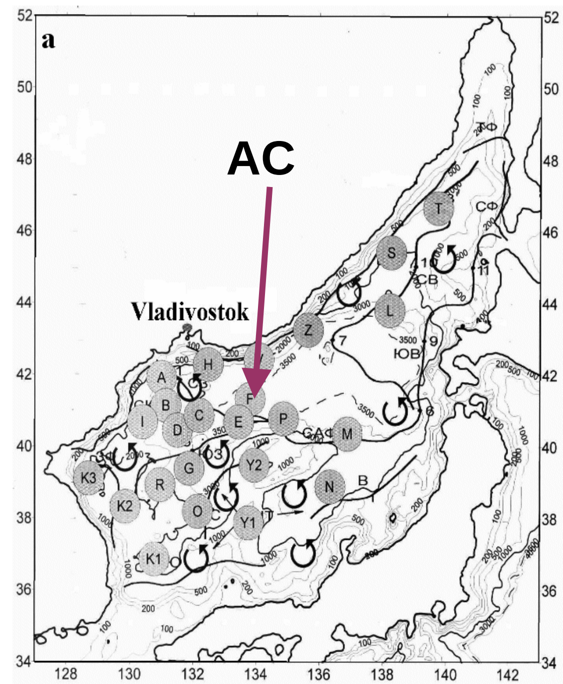

Intensified eddy formation in April and October (Nikitin, 2006)

The increase of Semiannual-Mode-related SST in the western core can be caused by northward shift of Subarctic Front in spring and intensified AC eddy formation in spring and autumn induced by the increased occurrence of AC wind stress curl.

Semiannual Mode: northern core

Temperature

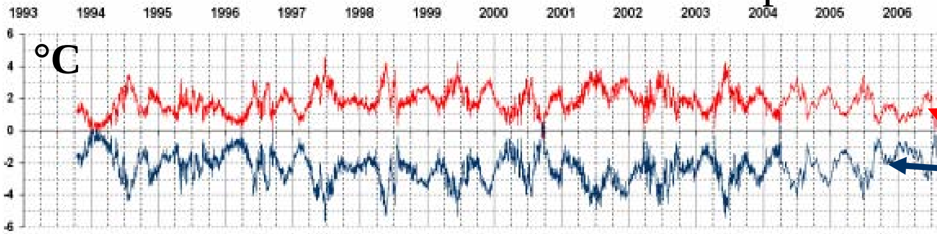

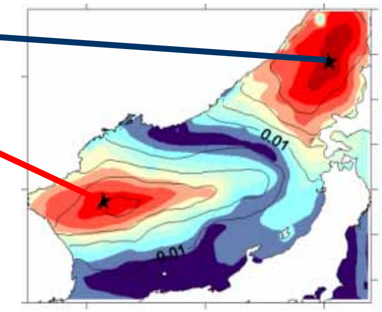

Why in opposition?

Westerlies

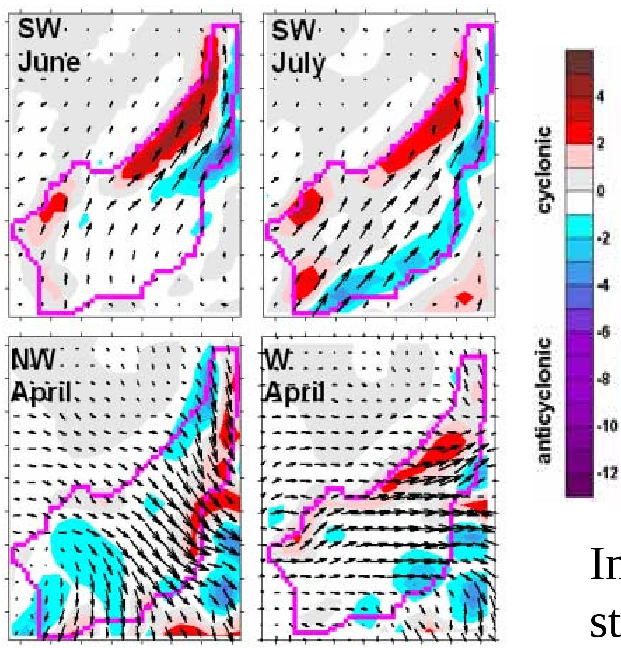

Easterlies

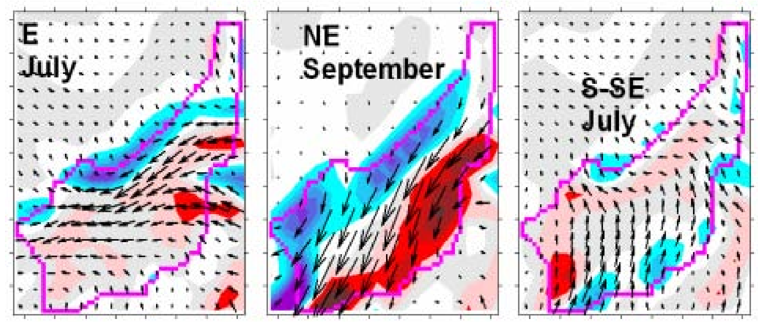

In the warm season, the occurrence of the C (AC) wind stress curl is increased for easterlies (westerlies), with the tendency of opposite curl over the central and northern JES

Changing curl can induce variety of circulation patterns in the northern JES

Circulation patterns in the northern JES

Sea surface height

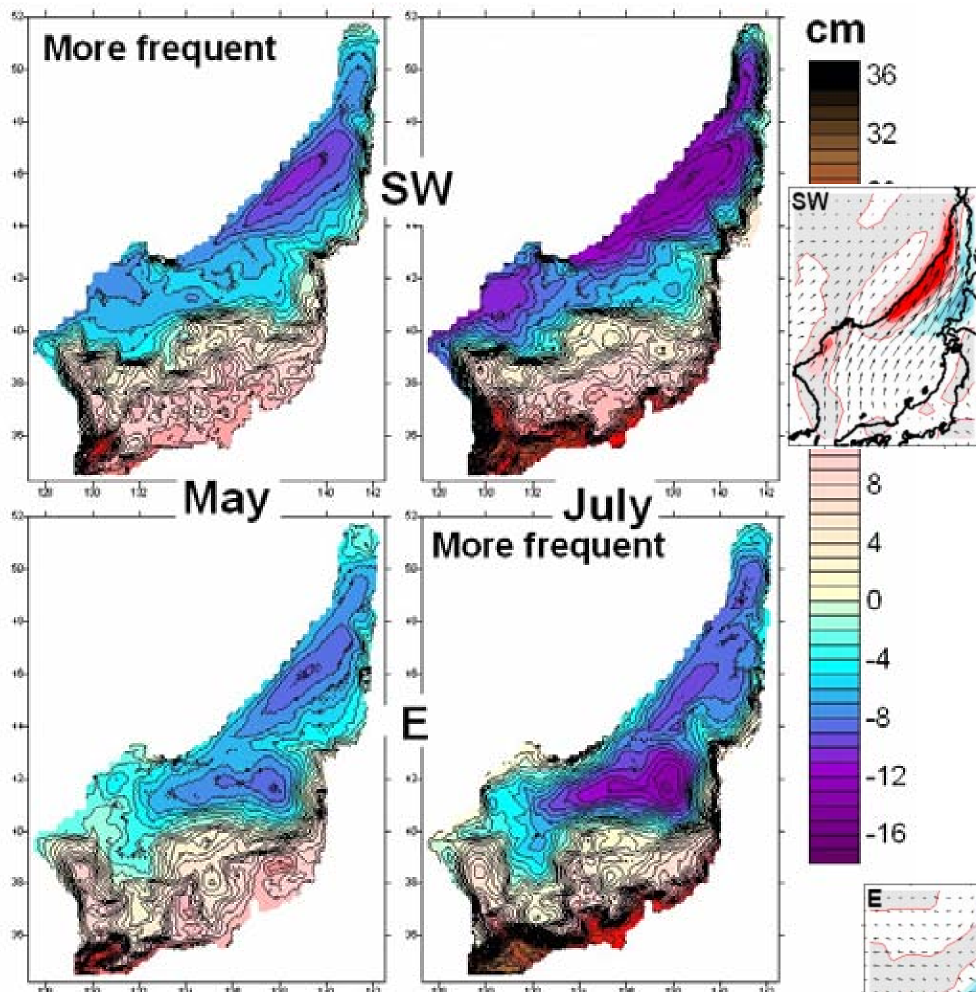

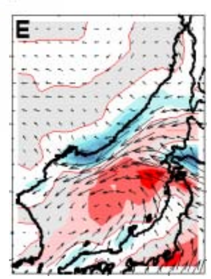

Opposite tendency in the strength of the C circulation in the northern and western JES

The cyclonic circulation in the northern JES strengthens (weakens) under the forcing of westerly (easterly) winds in opposition with the circulation in the central subarctic JES, inducing the opposite SST patterns.

Variety of observed circulation patterns (Dyakov, 2006);
AC eddies in the northern JES (Nikitin, 2005)

JMA SSTA2: Semiannual and Three Core Modes: spatial patterns

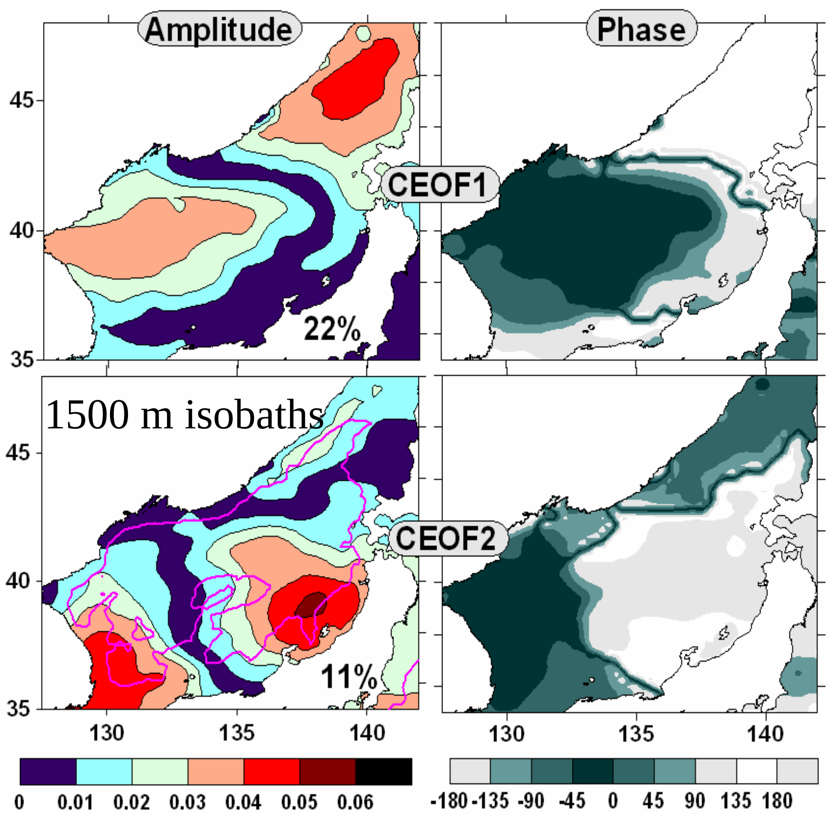

Second order residual anomalies obtained by subtraction of adjustment to the average annual cycle:
$\mathbf{X_a}^{(2)}(\mathbf{r}, t) = \mathbf{X_a}^{(1)}(\mathbf{r}, t) - A_1(\mathbf{r})B_1(t)$

JMA SSTA2 vs. JMA SSTA1 vs. NG SSTA2

Similar pattern for the *Semiannual Mode*; temporal pattern (not shown) also similar.

Three Core Mode:

- Korea Core centered in the SW JES;
- Honshu Core centered over the slope off mid Honshu in the Tsushima Current area;
- Primorye Core stretched over the continental slope in the Primorye (Liman) Current zone.

JMA SSTA2 Three Core Mode: temporal patterns

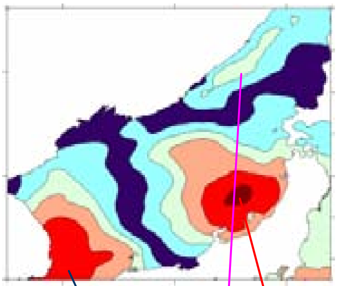

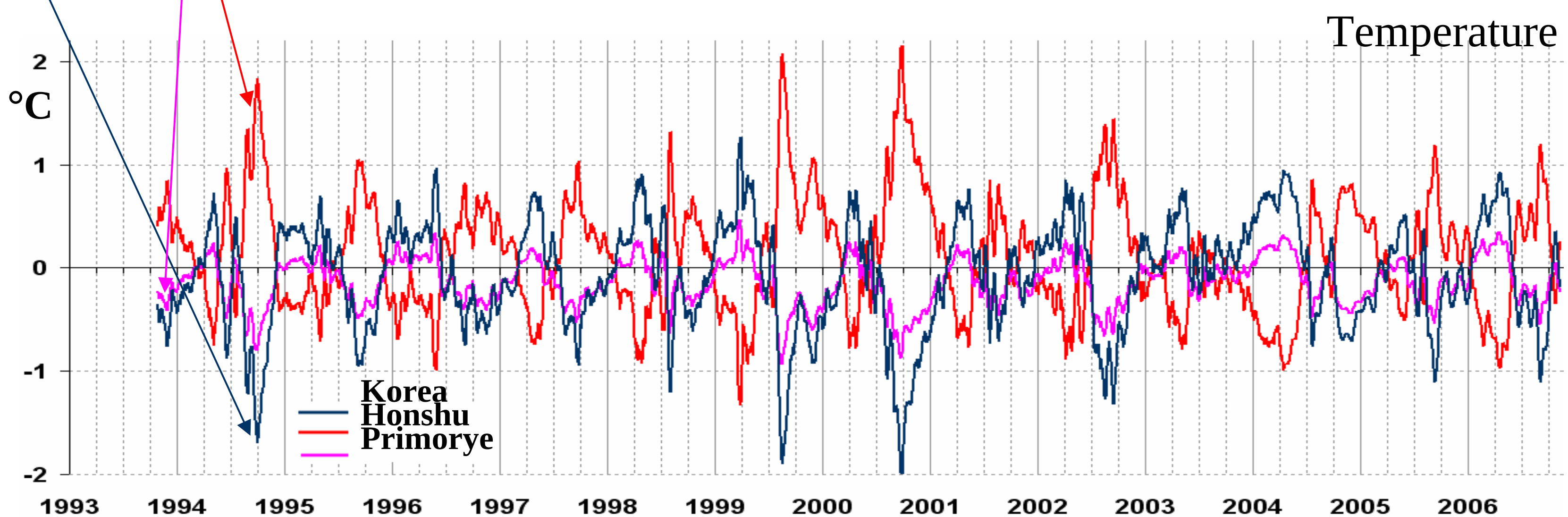

- Weaker anomalies than for the previous modes.
- Develop in August – September, sometimes from July, often persist through fall.
- Weaker anomalies of the opposite sign develop in spring.
- **Interannual variation**. *Strong summer – fall anomalies*: *1994, 1999, 2000, 2002.*

No summer – fall anomalies in 2003 →

accounts for the NG –JMA difference.

The JES circulation and JMA SSTA2 Three Core Mode

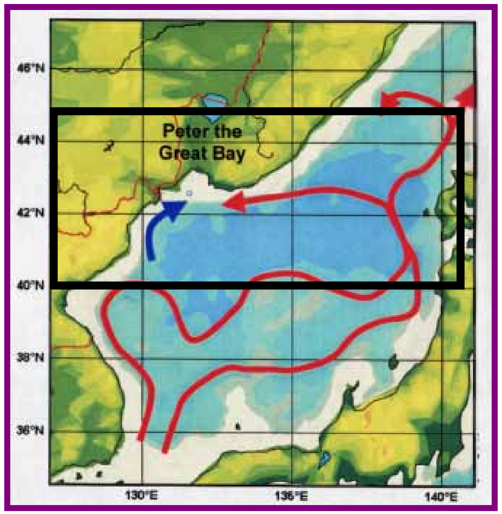

Scheme of transport of subtropical water towards the Primorye coast (Lobanov et al., 2001)

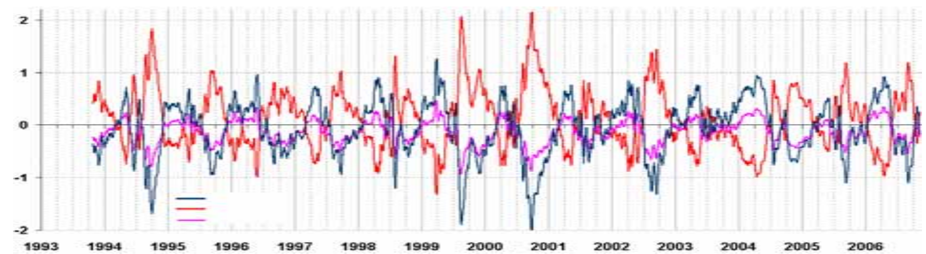

- Positive (negative) anomalies in the Honshu (Primorye) Core imply the strengthening of the Tsushima Current off mid Honshu and the Primorye Current off the NW coast.
- Negative anomalies in the Korea Core imply the weakening of the AC circulation in the western JES.
- Weaker anomalies of the opposite sign in spring imply the opposition of dynamic processes.
- **Interannual variation**. *Strong summer – fall anomalies*: *1994, 1999, 2000, 2002.*

1999-2001: the years of the weak or absent EKWC (Chang et al., 2004; Mitchell et al., 2005).

Currents in late summer simulated under the C wind stress curl

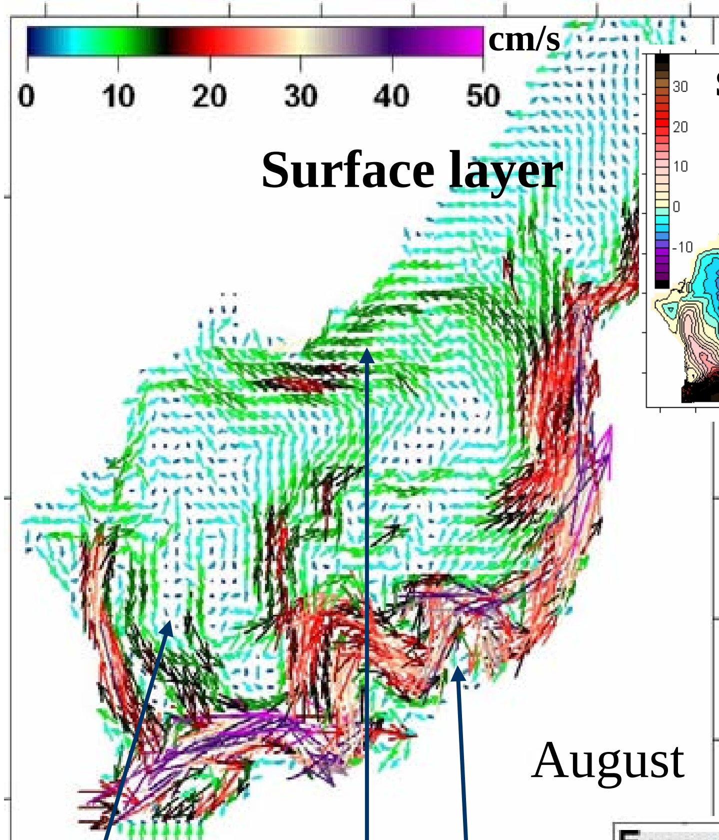

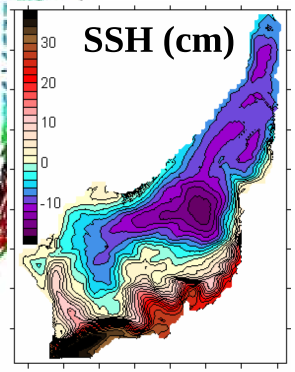

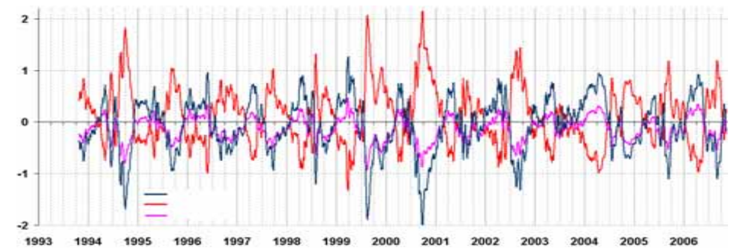

Occurrence of winds with the prevailing C curl

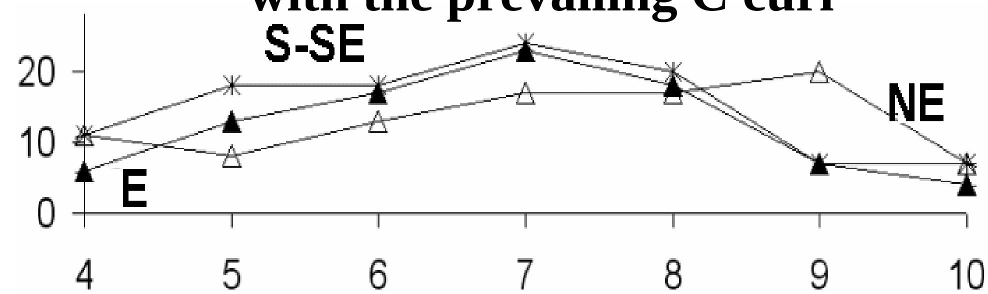

- Weakened AC circulation in the SW JES
- Intensified Tsushima Current off Honshu
- Intensified Primorye Current

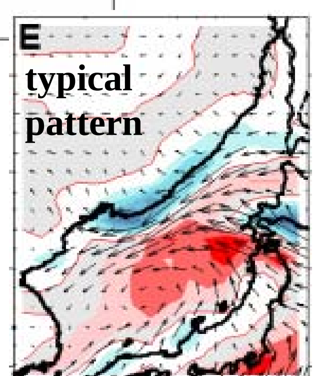

Interannual variation in not explained, as SSTA and C curl occurrence do not match explicitely on this timescale.

NG SSTA2 Three Core Mode: standing vs. propagating signal

Instantaneous SSTA
related to Three Core Mode

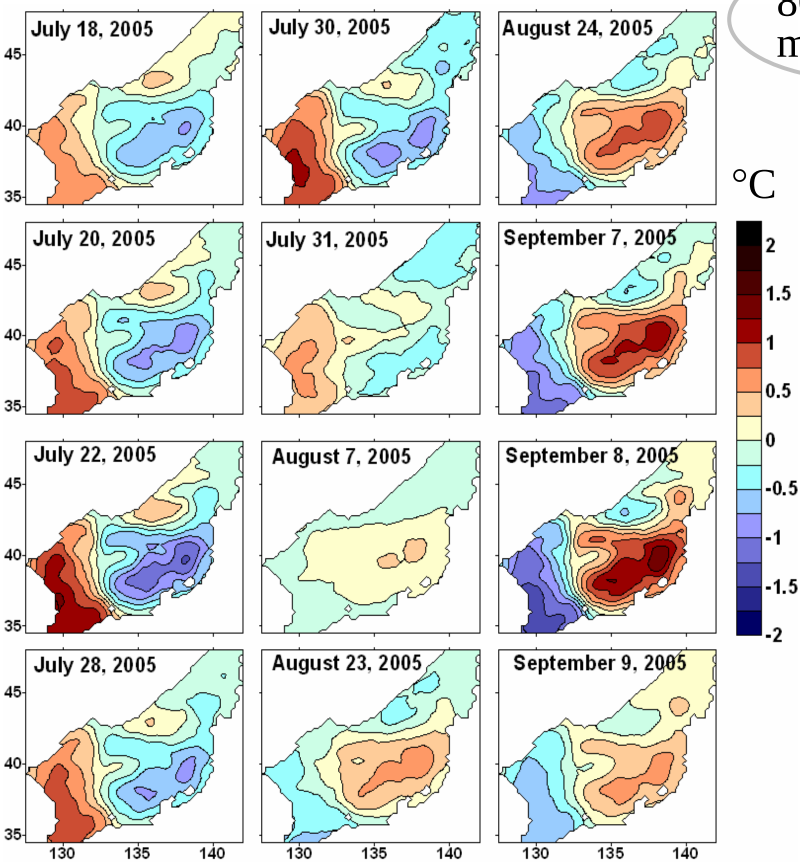

July 17, 2005 – September 9, 2005: strong standing oscillation and weak propagating anomalies

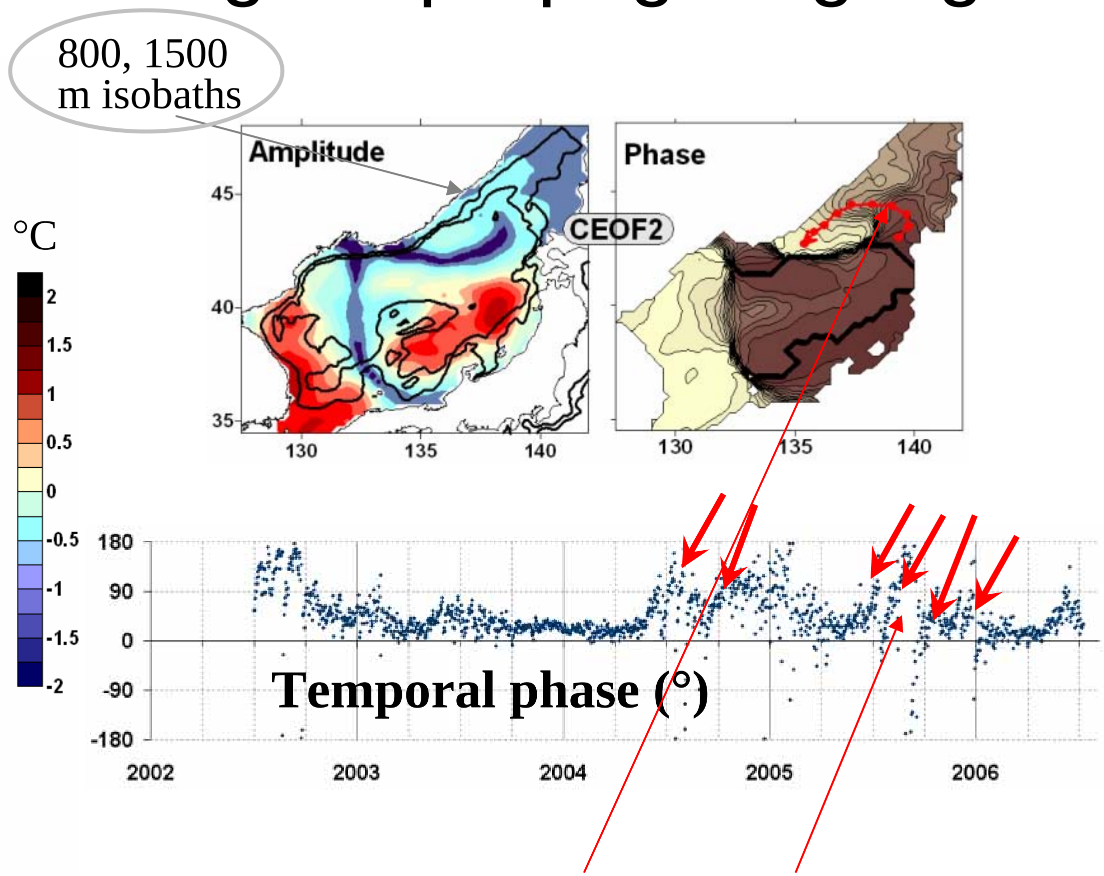

Gradual increase of the spatial and temporal phase: episods of anomaly propagation along the path of the western branch of the Tsushima Current with the speed of ~ 10 cm/s

Conclusion

•Dynamically induced anomalies are revealed in the JES SST after removal of the spatially averaged annual cycle accounting for the air – sea heat exchange variations.

•The responsible processes are the inflow of subtropical water from the Korea Strait, surface circulation divergence induced by Ekman suction, shifts of the western subarctic frontal system, AC eddy formation, wind-driven strengthening/weakening of currents.

•Annual timescales are revealed different from the annual cycle.

•A semiannual mode is revealed, lagging 2 months behind the increased occurrence of the AC/C wind stress curl.

•Episodic west – east anomaly propagation, mostly in late summer, is revealed from the Tsugaru Strait towards the Primorye coast along the path of the westward branch of the Tsushima Current.